J Mater Sci: Mater Med (2008) 19:899–906
DOI 10.1007/s10856-007-3007-8

Experimental investigation and theoretical modelling of the nonlinear acoustical behaviour of a liver tissue and comparison with a tissue mimicking hydrogel

Sergio Casciaro · Christian Demitri · Francesco Conversano · Ernesto Casciaro · Alessandro Distante

Received: 5 August 2006 / Accepted: 15 March 2007 / Published online: 1 August 2007
© Springer Science+Business Media, LLC 2007

Abstract Native harmonics generated by nonlinear distortion of ultrasound during propagation in a medium may cause misinterpretations in spectral analysis when studying contrast agents. The aim of this paper is to quantitatively evaluate nonlinear propagation effects of diagnostic ultrasound pulses in biological tissues and to assess whether a cellulose-based hydrogel can be a suitable material for tissue mimicking purposes. Hydrogel and pig liver tissue samples of various thicknesses were insonified in a through-transmission set-up, employing 2.25-MHz pulses with different mechanical index (MI) values (range 0.06–0.60). Second harmonic and first harmonic amplitudes were extracted from spectra of received signals and their ratio was then used to compare hydrogel and liver behaviours. Resulting trends are very similar for sample thicknesses up to 8 cm and highlight a significant increase in nonlinearity for MI > 0.3, for both liver and hydrogel. A numerical procedure was also employed to calculate pressure distribution along the beam axis: these theoretical results showed a very good agreement with experimental data in the low pressure range, though failed in predicting the MI threshold. In conclusion, the hydrogel resulted to be a suitable material for manufacturing tissue mimicking phantoms, in particular to study contrast agent behaviour with a "low power approach".

S. Casciaro (✉) · E. Casciaro · A. Distante
Institute of Clinical Physiology, National Council of Research, c/o Campus Ecotekne, via per Monteroni, Lecce 73100, Italy
e-mail: casciaro@ifc.cnr.it

S. Casciaro · C. Demitri · F. Conversano · A. Distante
Bioengineering Division, Euro Mediterranean Scientific Biomedical Institute, Brindisi, Italy

Introduction

During the last decade ultrasound (US) contrast agents, composed of gas microbubbles encapsulated by a shell of non-toxic material, have been widely used for a better delineation of the heart cavities [1], especially the left ventricle, for small vessels detection [2], for the assessment of tissue perfusion [3–5] and also for some tumor investigations [6–8]. Nowadays research in this field is directed towards more advanced applications, such as targeting, gene and drug delivery, and this has recently increased, in particular, the interest in nonlinear propagation and scattering of US waves in human tissues [9, 10].

In fact, it is now well established that the achievement of optimal and successful use of ultrasound contrast agents requires in vitro attenuation and scattering experiments to be performed on a wide range of parameter settings and the introduction of new signal processing techniques based on the radiofrequency (RF) signal analysis [5, 11–13].

One of these techniques is the harmonic imaging [14–16], which has already been incorporated in a number of commercially available echographic scanners. Harmonic imaging exploits the nonlinear behaviour of the contrast agents when perfusing a tissue: for certain pressure amplitudes and frequencies of the applied ultrasound, microbubbles oscillate in a nonlinear manner introducing harmonics in the scattered signal [17]. The second harmonic component, in particular, often results to be of considerable intensity. In fact, the general concept of

harmonic imaging is selectively filtering of the second harmonic component, whose amplitude is displayed and claimed to show only the presence of the contrast agent [18]. Applying such a method, the detection of very low perfusions in tissues becomes feasible [19].

Many previous studies reported impressive harmonic responses of contrast agents [14, 15, 20–22], but in some cases it remains unclear the interaction between these harmonics and surrounding tissues. Recently, in fact, a novel imaging concept (native harmonic imaging) was introduced as a technique capable of displaying the harmonic components generated by ultrasound propagating in tissue (native harmonics) [23]. The generation of measurable native harmonics by nonlinear ultrasound distortion in tissue indicates that care should be taken when interpreting the harmonic signals from contrast agent measurements. Measured harmonic signals, in fact, could represent a mixture of the tissue native harmonic signals and of the contrast agent intrinsic harmonic signals.

Another possible source of harmonics which is not explicitly mentioned in many studies is the incident ultrasound signal itself, which can contain harmonics generated by the transducer [18]. For example, many commercial systems employ a square wave activation signal which contains itself strong uneven harmonic components and this might again influence the interpretation of harmonic signals.

Hence, in summary, in every ultrasound investigation involving contrast agents, harmonics may originate from three possible sources: microbubble intrinsic harmonics, tissue native harmonics generated by nonlinear distortion of ultrasound during propagation and contaminating harmonics contained in the ultrasound signal itself [18].

It is evident that these phenomena must be taken into account in particular when performing in vitro studies aimed to the characterization of nonlinear behaviour of experimental ultrasound contrast agents. This means that materials to be employed in the manufacturing of tissue mimicking phantoms should be chosen not only based on the values of their density, speed of sound and attenuation coefficient, but also considering their effect on the appearance of native harmonics during ultrasound propagation through them.

The purpose of this paper is a quantitative evaluation of nonlinear propagation effects of diagnostic ultrasound pulses in a biological tissue and to assess whether a cellulose-based hydrogel (having values of acoustic attenuation coefficient and speed of sound very close to those of the studied tissue) can be considered a suitable material also for simulating nonlinear propagation effects. Experimental results have been also compared with data obtained from numerical calculations applied to both liver and hydrogel.

Materials and methods

Cellulose-based hydrogel synthesis and characterization

A cellulose-based hydrogel was synthesized in a partially swollen state by cross-linking water solutions of carboxymethylcellulose sodium salt (CMCNa) and hydroxyethilcellulose (HEC). Divinylsulfone (DVS) was used as a cross-linking agent. The total polymer weight fraction in the solution was 2%. CMCNa, HEC and DVS were purchased from Aldrich Chemical (Aldrich Chemical Company Inc. Milwaukee, WI) and used as received. The presence of HEC is necessary to promote quantitatively intermolecular rather than intramolecular cross-linking. Cross-linking reaction was performed according to procedures reported in the literature [24]. After the mixing stage, an alkaline water solution of potassium hydroxide (KOH) was added as a catalyst. Hydrogel formation occurred at room temperature after 12–14 h.

The described production process was performed in order to obtain the same values of sound velocity and attenuation coefficient described in literature for liver tissue [25]. Different hydrogel samples were prepared by varying the weight ratio between CMCNa, HEC and DVS. Sound velocity and attenuation coefficient were calculated for each producted sample through ultrasound analysis. Density measurements were also performed on every sample. The sample whose properties were found to be the closest to the reference values was chosen to undergo the investigation described in the next paragraphs.

Pig liver preparation

Pig liver was selected for its properties very similar to human liver [26]. The samples to investigate were excised a few minutes before measurements immediately after slaughter, and kept at room temperature. This tissue was chosen as reference in order to compare its harmonic behaviour with the corresponding of the cellulose-based hydrogel.

Experimental setup and measurement procedure

Figure 1 shows the experimental apparatus used to study the harmonic tissue behaviour. A programmable function generator (TG1010A 10 MHz D.D.S., Thurlby Thandar Instruments Ltd., Huntingdon, U.K.) provided the generation of square wave pulses composed of 10 cycles at the frequency of 2.25 MHz, with a pulse repetition frequency (PRF) of 10 Hz. These signals were first amplified in an inverting broadband RF power amplifier (FLL-75, Frankonia MV-Mess-Systeme GmbH, Heideck, Germany)

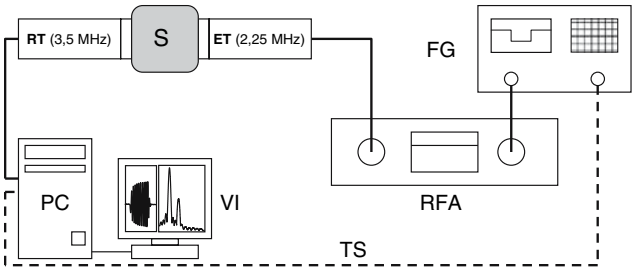

Fig. 1 Scheme of the measuring system. (S = Sample; ET = Emitter Transducer; RT = Receiver Transducer; FG = Function Generator; RFA = Radio Frequency Amplifier; TS = Trigger Signal; PC = Personal Computer; VI = Virtual Instrument)

and then supplied to an unfocused 2.25-MHz ultrasound transducer with a diameter of 12.7 mm (V306, Panametrics, Olympus NDT, Waltam, MA). An example of employed ultrasound signal and corresponding spectrum is reported in Fig. 2.

The square wave pulse was chosen, according to the transducer manufacturer technical notes, for its suitability at high number of cycles and high voltages. Considering the harmonic frequencies involved in this study, it was not possible to detect exactly the second harmonic component using a receiving transducer having the same center frequency of the transmitting one. So, the use of a receiver with a frequency characteristic shifted towards higher values allowed the correct detection of second harmonic component. This benefit is limited by the receiver characteristics and a correction on received signal spectrum was required. This correction, in our case, was achieved through a custom designed software tool, realized with LabView™ (National Instruments Corporation, Austin, TX), that implemented the spectral correction based on the broadband FFT spectrum of the probe [23].

Signals transmitted through the samples were received by a 3.5-MHz unfocused ultrasound transducer (V382, Panametrics, Olympus NDT, Waltam, MA), that was connected to a computer via a data-acquisition board (PCI-5122, National Instruments Corporation, Austin, TX) used to digitize (100 MHz, 14 bits) the signals, that were then stored in the computer hard disk for off-line analysis. The function generator and the data transfer were controlled by a virtual instrument (VI) realized with LabView™. The same software was also employed to implement the needed algorithms for off-line data analysis.

Our measurements were planned to study the onset of native harmonics in both pig liver and hydrogel varying MI value and sample thickness. In particular, we focused our attention on the appearance of second harmonic, that was assessed through the calculation of the ratio H2/H1, where H1 and H2 represent respectively first harmonic and second harmonic amplitude extracted from the received signal spectra.

In order to study the MI effect, we chose to insonify two sample thicknesses (3 cm and 6 cm, that represent penetration depths typically encountered in phantom studies involving ultrasound contrast agents) employing 19 different MIs (range 0.06–0.57) for each sample thickness.

In the second part of the experiment we evaluated the onset of native harmonics as a function of the penetration depth, again comparing liver and hydrogel behaviours through the calculation of the ratio H2/H1, with the specific goal of determining the maximum hydrogel thickness useable to effectively simulate liver tissue in phantom studies. In this case we chose 6 MI steps covering the range previously investigated (MI = 0.1, 0.2, 0.3, 0.4, 0.5, 0.6) to insonify 7 samples of different thicknesses ranging from 5 to 11 cm.

The digitized signals were further processed using a LabView™ custom designed software tool, that performed the correction of the acquired signal spectra and calculated the ratio H2/H1, where the values of H1 and H2 were obtained averaging 60 spectra derived from a sequence of consecutively acquired signals.

Determination of mechanical indices

The mechanical index (MI) is an important parameter for sonographers in the common clinical practice. MI is related to the acoustic pressure according to the following equation:

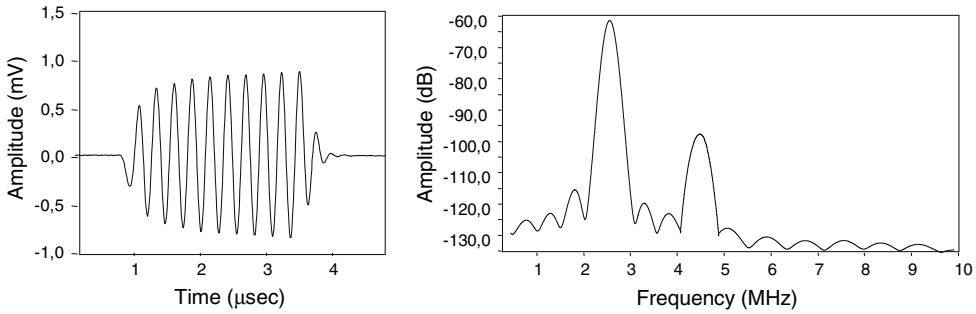

Fig. 2 Ultrasound pulse (10 cycle; 2.25 MHz) measured in water and its FFT spectrum

$$MI = \frac{Pa}{\sqrt{f}} \quad (1)$$

where Pa and f are respectively the acoustic pressure measured in the matter and the wave frequency. Since most commercially available echographs present a manual control of MI only, this parameter became our reference in the study, in order to facilitate the comparison of our experimental results with clinical assessments of contrast media.

The MI range calculation was performed by employing a 0.5-needle hydrophone (uncertainty 14%, sensitivity 512.3 mV/MPa, Precision Acoustic Ltd, Dorchester, UK). The transducer was driven by a 10-cycle square wave pulse at 2.25 MHz, produced by the function generator connected to the RF amplifier. The driving signal amplitude was then varied in order to obtain the above mentioned steps of MI. A digital oscilloscope (TDS 2014, Tektronix Inc. Beaverton, OR) provided both the visualization and the storage of the received signal. By using Eq. (1) we calculated MI values starting from acoustic pressures measured through the needle hydrophone.

Numerical model

The theoretical model described in this paragraph is based on the theory of a plane ultrasound wave. In order to verify the applicability of this theory, the pressure distribution in the beam has been measured to define the boundary conditions on the transducer surface. Measurements were taken to get the radial pressure profile varying the distance from the transducer. The basic assumption for the pressure profile on the transducer surface is taking for that the pressure measurement closest to the surface itself. The needle hydrophone and the 2.25-MHz transducer were employed for these measurements too. This choice has been supported by the fact that a good agreement was found between the measured radial pressure distribution and the analytical curve $[1–(r/a)^6]$ usually chosen as an approximation for pressure distribution on the transducer surface (z = 0 cm), where r is the radial coordinate and a the transducer radius [23].

In literature, many numerical models predicted accurately nonlinear pressure field of diagnostic US, showing a good agreement with experimental measurements performed in water [23, 27–29]. Some of these studies compared also theoretical model results with experimental data in a propagation medium other than water (e.g. soft tissues and biological fluids).

The following equations [18] give an approximation of the acoustic pressure amplitudes of H1 and H2 for a monochromatic finite amplitude plane wave travelling through a medium as a function of the distance (z) from the source:

$$p_2(z) = \frac{(1 + B/2A) \cdot \pi \cdot f}{\rho \cdot c^3} \cdot p_1^2(0) \cdot z \cdot e^{-(\alpha_1 + \frac{\alpha_2}{2}) \cdot z} \quad (2)$$

$$p_1(z) = p_1(0) \cdot e^{-\alpha_1 \cdot z} \quad (3)$$

Here $p_1(0)$ is the amplitude of H1 at the transducer surface, $1 + B/2A$ is the coefficient of nonlinearity (B/A is the nonlinearity parameter), ρ (kg/m^3) and c (m/s) are respectively the density and the sound velocity of the investigated medium, f (Hz) is the ultrasonic frequency applied, α_1 and α_2 are the attenuation coefficients for H1 and H2 respectively. Equation (2) takes into account the assumption that for most biological tissue the linear dependence between the attenuation coefficient and frequency ($\alpha_2 = 2\alpha_1$) is valid [30, 31].

Theoretical values of H2/H1 were calculated using Eqs. (2) and (3) for an ultrasound pulse of 2.25 MHz propagating in liver tissue [$\alpha_1 = 8.5 \times 10^{-2}$ Np/(cm × MHz), $\alpha_2 = 1.7 \times 10^{-1}$ Np/(cm × MHz), B/A = 7.2, $\rho = 1.03 \times 10^3$ kg/m^3, $c = 1560$ m/s] and in hydrogel [$\alpha_1 = 6.7 \times 10^{-2}$ Np/(cm × MHz), $\alpha_2 = 1.34 \times 10^{-1}$ Np/(cm × MHz), B/A = 10.3, $\rho = 1.03 \times 10^3$ kg/m^3, $c = 1560$ m/s]. Results coming from this numerical calculation have been compared with those experimentally obtained, as described in the next section.

Results and discussion

Experimental data

We investigated the nonlinear propagation effects of diagnostic ultrasound in pig liver tissue and hydrogel insonifying samples of various thicknesses with 10-cycle pulses at the frequency of 2.25 MHz and employing different MI values. The appearance of native harmonics was assessed for both materials referring to the ratio H2/H1 extracted from the received signal spectra.

In particular, we studied separately the effect of MI value and penetration depth on the onset of native harmonics. For the first objective, we chose two sample thicknesses (3 cm and 6 cm) and insonified the corresponding samples employing 19 different MIs (range 0.06–0.57).

Obtained plots of H2/H1 against MI for both liver tissue and hydrogel are reported in Figs. 3 and 4, respectively for 3-cm and 6-cm sample thickness. It is evident from the graphs that nonlinear propagation effects increase with MI for both liver tissue and hydrogel for each tested penetration depth. For each employed MI value the ratio H2/H1 results higher for hydrogel than for liver tissue, but trends showed by hydrogel curves are very close to those of the corresponding liver ones and the two materials present a

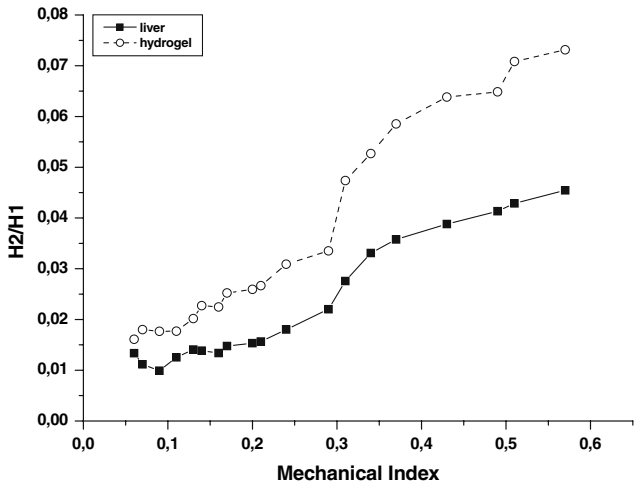

Fig. 3 Plot of experimentally measured H2 to H1 ratio for liver and cellulose-based hydrogel against MI value (3-cm sample thickness; 10-cycle pulses; 2.25-MHz US frequency; PRF = 10 Hz)

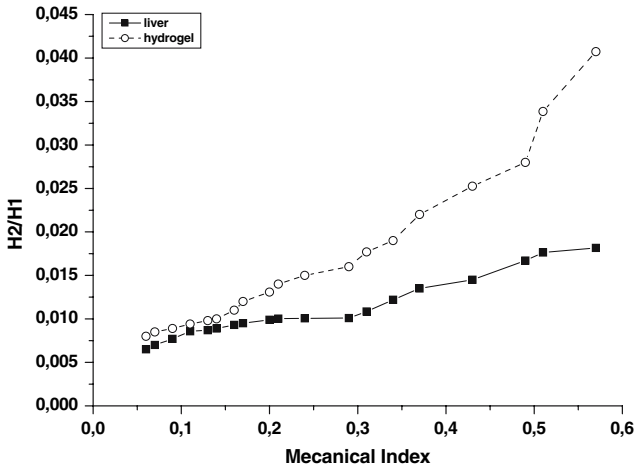

Fig. 4 Plot of experimentally measured H2 to H1 ratio for liver and cellulose-based hydrogel against MI value (6-cm sample thickness; 10-cycle pulses; 2.25-MHz US frequency; PRF = 10 Hz)

very similar behaviour, especially in the low MI range. It is also interesting to note the presence of a kind of nonlinear threshold around MI = 0.3: above this value both materials show a marked increase in H2/H1, which is more evident in Fig. 3 (3-cm sample thickness) but is still visible in Fig. 4 (6-cm sample thickness). These data indicate that generation of native harmonics in the liver increases considerably for MI > 0.3, so suggesting that an optimization in the contrast harmonic imaging techniques in the liver for MI < 0.3 is possible, since the amount of native harmonics is negligible and misinterpretations could be consequently avoided.

In fact, it is known [32] that energy redistribution among frequency components in the ultrasound beam during propagation, which causes the onset of native harmonics, becomes evident for "large" oscillations of medium molecules, while this effect can be neglected for corresponding small amplitude waves. The ultrasound amplitude threshold that produces the appearing of harmonic components in the propagating signal, then, depends on the molecular structure and microarchitecture of the medium. Our results suggest that, in the case of liver, specific nonlinear characteristics of the tissue give such an amplitude threshold around MI = 0.3.

It is important to underline that the described MI threshold in the liver acoustic behaviour is perfectly reproduced by the hydrogel, therefore it results a very suitable candidate for manufacturing phantoms for in vitro studies aimed to improve the use of ultrasound contrast agents in liver examinations. In particular, the fact that, as showed in Figs. 3 and 4, H2/H1 ratio is always higher for hydrogel than for liver (in most of cases is approximately twice as high) can be considered an advantage when performing in vitro studies of contrast microbubble harmonic behaviour. In fact, once microbubbles have been demonstrated in vitro to produce useful harmonic components (i.e., higher than those generated by the hydrogel in absence of contrast particles), then their effectiveness in vivo will be definitely better, given the lower harmonic contribution of liver tissue with respect to hydrogel. Moreover, it will be always possible to accurately estimate a priori the in vivo achievable harmonic enhancement, thanks to the exact knowledge of the differences in harmonic generation between hydrogel and liver tissue.

Furthermore, we can observe that curves reported in Fig. 4, although qualitatively presenting the same trends of their corresponding in Fig. 3, are characterized by lower values of H2/H1. This, in principle, could be caused by two different phenomena: (1) the appearance of higher harmonics in the case of deeper samples; (2) the exponential increase of attenuation with penetration depth, which is always more noticeable for higher frequency components. By studying the penetration depth effect, as described in the following, we verified that the appearance of considerable higher harmonics requires propagation paths longer than 9 cm. Therefore, observed differences between curves reported in Figs. 3 and 4 are more probably due to the fact that, increasing the penetration depth from 3 cm to 6 cm, second harmonic attenuation grows more rapidly than further second harmonic generation caused by nonlinear effects.

In the second part of the experiment we evaluated the onset of native harmonics as a function of the penetration depth, again comparing liver and hydrogel behaviours through the calculation of the ratio H2/H1, with the specific goal of determining the maximum hydrogel thickness useable to effectively simulate liver tissue in phantom studies.

Data obtained for MI = 0.1 are plotted in Fig. 5. Reported graphs emphasize a substantial coincidence of liver and hydrogel behaviour until a sample thickness of 8 cm, while, for higher penetration depths, the hydrogel curve shows a clear maximum at 9 cm and then it decreases, but remains quite higher than the liver curve.

These different trends can be explained as follows. In the first part of the curve, native harmonic generation increases with penetration depth for both hydrogel and liver, but the increasing rate is higher in the hydrogel and this causes the progressive separation of the two curves, that becomes evident above 8 cm. In correspondence of a sample thickness of 9 cm the amplitude of second harmonic generated in the hydrogel reaches its maximum and then it shows a drop, probably due to the appearance of higher harmonics. The same phenomenon is present in the liver case but it appears less pronounced, resulting in the different behaviour showed by hydrogel and liver for sample thicknesses above 8 cm.

Results obtained for higher MI values are reported in Figs. 6 and 7. These plots confirm the behaviours observed in Fig. 5, showing in particular that, for higher MI, the hydrogel peak at 9 cm becomes more evident. As mentioned before, increasing penetration depth causes the increase of both attenuation and harmonic production, with the latter being also augmented in presence of higher MI values. These two phenomena affect ultrasound propagation through hydrogel and liver tissue in slightly different ways: harmonic generation due to nonlinear ultrasound distortion clearly dominates inside the hydrogel for penetration depths higher than 6 cm, while in the case of liver tissue ultrasound distortion is better balanced by attenuation effects. However these differences become quantitatively evident only for penetration depths of at least 9 cm, where second harmonic generation in the hydrogel reaches its maximum. Further increases in penetration depth, with consequent further signal distortion, are likely to cause the appearance of higher harmonics in the propagating pulse, producing the observed drop in H2/H1 value. This takes place for propagation paths longer than 9 cm in the hydrogel and longer of 8 cm in the liver. So we can conclude that the differences between hydrogel and liver become significant for penetration depths higher than 8 cm and at higher MIs. On the other hand, then it is clearly demonstrated that hydrogel represents a fine approximation of the liver behaviour for thicknesses smaller than 8 cm

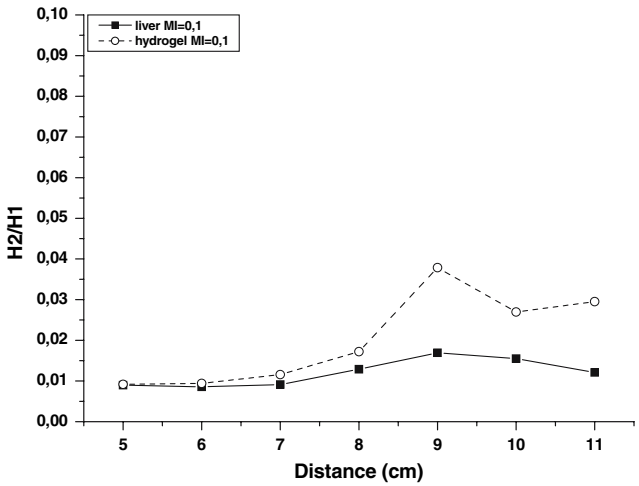

Fig. 5 Plot of experimentally measured H2 to H1 ratio for liver and cellulose-based hydrogel against sample thickness (MI = 0.1; 10-cycle pulses; 2.25-MHz US frequency; PRF = 10 Hz)

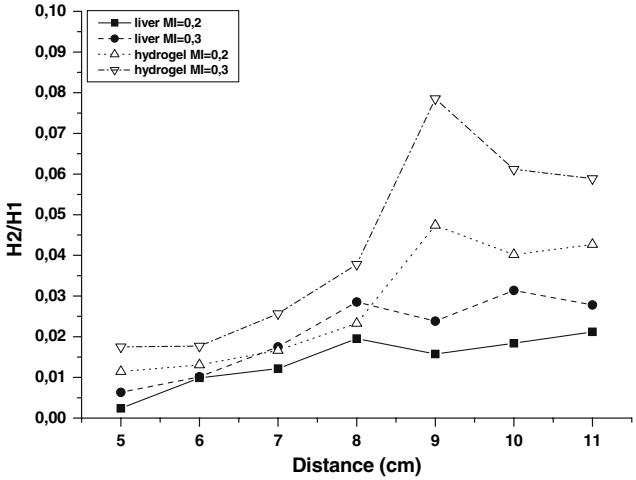

Fig. 6 Plot of experimentally measured H2 to H1 ratio for liver and cellulose-based hydrogel against sample thickness (MI = 0.2, MI = 0.3; 10-cycle pulses; 2.25-MHz US frequency; PRF = 10 Hz)

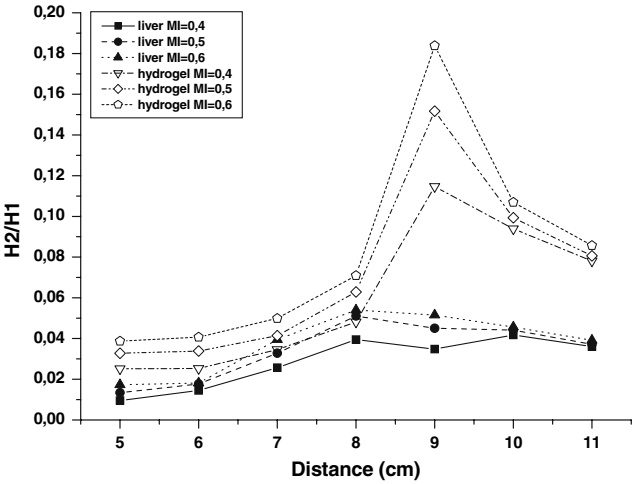

Fig. 7 Plot of experimentally measured H2 to H1 ratio for liver and cellulose-based hydrogel against sample thickness (MI = 0.4, MI = 0.5, MI = 0.6; 10-cycle pulses; 2.25-MHz US frequency; PRF = 10 Hz)

and the goodness of this approximation increases markedly for low MI values.

Numerical calculation results

The theoretical model described in the previous section was applied to calculate the pressure distribution of the first and second harmonic along the beam axis, both inside the liver and the hydrogel. In this way we obtained theoretical values of the ratio H2/H1, that were compared with those experimentally measured for a 3-cm sample thickness (reported in Fig. 3). Theoretical values of H2/H1 were calculated using Eqs. (2) and (3) for an ultrasound pulse of 2.25 MHz propagating in liver tissue and in hydrogel.

Calculated results and measured data are reported in Figs. 8 and 9, respectively for liver tissue and hydrogel. For both materials there is a good agreement between experimental data and numerical calculations until MI = 0.3, that is as long as native second harmonic increases approximately in a linear manner with MI, while for MI > 0.3 the harmonic increasing rate rises, as observed and discussed in the previous paragraph, while the model still predicts a linear increase for the whole tested MI range.

The assessment and development of possible improvements of this model for higher MI range will be the objective of future studies.

Conclusions

This study evaluated nonlinear propagation effects of diagnostic ultrasound in pig liver tissue and in a cellulose-based hydrogel, the latter to be assessed as a candidate for the manufacturing of liver tissue mimicking phantoms. The onset of native harmonics in both materials was studied independently as a function of the incident MI and of the penetration depth.

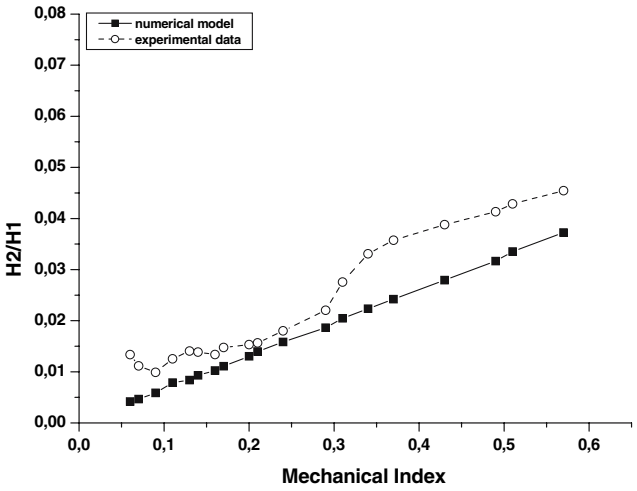

Fig. 8 Comparison between experimentally obtained and numerically calculated H2/H1 values plotted against MI for pig liver tissue (3-cm sample thickness)

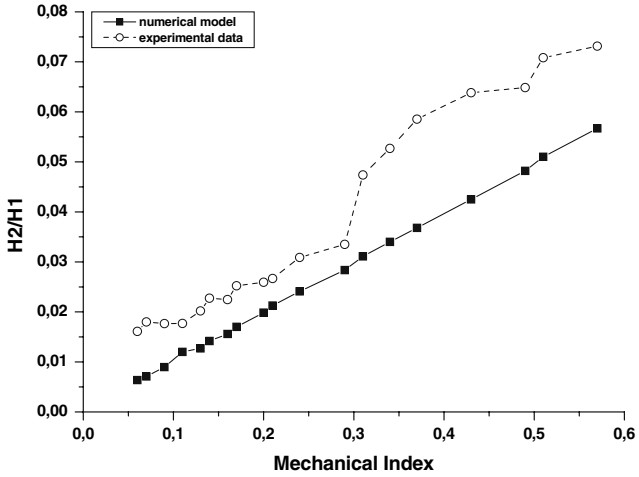

Fig. 9 Comparison between experimentally obtained and numerically calculated H2/H1 values plotted against MI for cellulose-based hydrogel (3-cm sample thickness)

Presented results demonstrated that the generation of native harmonics in the liver increases with MI, showing an onset for MI equal to 0.3. These findings suggest that contrast harmonic imaging techniques in the liver can be optimized for MI < 0.3, where the amount of tissue harmonics is negligible and artefacts on the corresponding echographic images could be significantly reduced.

Moreover, cellulose-based hydrogel resulted to be a very suitable candidate to in vitro simulate the nonlinear ultrasound propagation in liver tissue for penetration depths up to 8 cm. In particular, the hydrogel reproduced perfectly the MI threshold found for the liver harmonic onset and the goodness of the fit between liver and hydrogel behaviours is considerably better for MI < 0.3.

Experimental data were also compared with numerical calculation results, for both liver tissue and hydrogel. The adopted theoretical model showed a good agreement with measured data until MI = 0.3, but failed in predicting the described MI threshold, suggesting the need for further improvements of the model.

In conclusion, the studied cellulose-based hydrogel could be very useful in the manufacturing of tissue mimicking phantoms designed for the development of new low-power contrast harmonic imaging techniques for liver examinations. Synthesis technique adopted for the tested hydrogel also presents the possibility to be modulated in order to obtain new hydrogels, to accurately simulate acoustic linear and nonlinear properties of different organs and tissues.

Acknowledgements The authors thank Prof. Alfonso Maffezzoli and Dr. Alessandro Sannino for providing useful suggestions and guidance in the hydrogel synthesis and preparation. This work was partially funded by the FIRB-US RBNE01E9ZR and CERSUM Laboratory Rif. Min. Decreto Direttoriale 1105/2002 N° 243 granted by the Italian Ministry of Research.

References

1. A. L. STRAUSS and K. D. BELLER, *Ultrasound Med. Biol.* **23** (1997) 975
2. G. SEIDEL and M. KAPS, *Stroke* **28** (1997) 1610
3. L. J. BOS, *The Application of Contrast Echocardiography for the Assessment of Myocardial Perfusion* (Amsterdam: University of Amsterdam, 1997)
4. C. FRISCHKE, J. R. LINDNER, K. WEI, N. C. GOODMAN, D. M. SKYBA and S. KAUL, *Circulation* **96** (1997) 959
5. R. LEISCHIK, J. ROSE, G. CASPARI, A. SKYSCHALLY, G. HEUSCH and R. ERBEL, *Herz* **22** (1997) 40
6. P. HAUFF, T. FRITZSCH, M. REINHARDT, W. WEITSCHIES, F. LUDERS, V. UHLENDORF and D. HELDMANN, *Invest. Radiol.* **32** (1997) 94
7. Y. KONO, F. MORIYASU, Y. MINE, T. NADA, N. KAMIYAMA, Y. SUGINOSHITA, T. MATSUMURA, K. KOBAYASHI and T. CHIBA, *Invest. Radiol.* **32** (1997) 120
8. H. MADJAR and J. JELLINS, *Eur. J. Ultrasound* **5** (1997) 65
9. F. A. DUCK, *Ultrasound Med. Biol.* **28** (2002) 1
10. M. BENNET, S. MCLAUGHLIN, T. ANDERSON and N. MCDICKEN, *Ultrasound Med. Biol.* **31** (2005) 1051
11. M. J. MONAGHAN, J. M. METCALFE, S. ODUNLAMI, A. WAALER and D. E. JEWITT, *Eur. Heart J.* **14** (1993) 1200
12. B. WILSON, K. K. SHUNG, B. HETE, H. LEVENE and J. L. BARNHART, *Ultrasound Med. Biol.* **19** (1993) 181
13. A. BOUAKAZ, S. FRIGSTAD, F. J. TEN CATE and N. DE JONG, *Ultrasound Med. Biol.* **28** (2002) 59
14. P. N. BURNS, *Clin. Radiol.* **51** (1996) 50
15. P. H. CHANG, K. K. SHUNG, S. WU and H. B. LEVENE, *IEEE Trans. Ultrason. Ferroelectr. Freq. Control* **42** (1995) 1020
16. B. SCHROPE, V. L. NEWHOUSE and V. UHLENDORF, *Ultrason. Imaging* **14** (1992) 134
17. N. DE JONG, *Acoustic Properties of Ultrasound Contrast Agents* (Rotterdam: Erasmus University, 1993)
18. X. A. A. M. VERBEEK, J. M. WILLIGERS, P. J. BRANDS, L. A. F. LEDOUX and A. P. G. HOEKS, *Ann. Biomed. Eng.* **27** (1999) 670
19. M. BRUCE, M. AVERKIOU, K. TIEMAN, S. LOHMAIER, J. POWERS and K. BEACH, *Ultrasound Med. Biol.* **30** (2004) 735
20. P. D. KRISHNA and V. L. NEWHOUSE, *Ultrasound Med. Biol.* **23** (1997) 453
21. J. E. POWERS, P. N. BURNS and J. SOUQUET, *Advances in Echo Imaging using Contrast Enhancement* (Dordrecht: Kluwer Academic, 1997), p. 139
22. W. ZHENG and V. L. NEWHOUSE, *Ultrasound Med. Biol.* **24** (1998) 513
23. L. FILIPCZYNSKI, J. WOJCIK, T. KUJAWSKA, G. LYPACEWICZ, R. TYMKIEWICZ and B. ZIENKIEWICZ, *Ultrasound Med. Biol.* **27** (2001) 251
24. A. SANNINO, A. ESPOSITO, L. NICOLAIS, M. A. DEL NOBILE, A. GIOVANE, C. BALESTRIERI, R. ESPOSITO and M. AGRESTI, *J. Mater. Sci. Med.* **11** (2000) 247
25. M. BAZZOCCHI, *Ecografia*, 2nd edn. (Idelson Gnocchi, 2001)
26. S. CASCIARO, C. DEMITRI, R. PALMIZIO ERRICO, F. CONVERSANO, G. PALMA, E. CASCIARO and A. DISTANTE, In *Proceedings of the IEEE International Ultrasonics Symposium, Rotterdam, September 2005*, edited by M. Passini Yuhas (Aurora, IL: Industrial Measurement System, 2005), p. 1668
27. S. I. AANONSEN, T. BARKVE, J. N. TJOTTA and S. TJOTTA, *J. Acoust. Soc. Am.* **75** (1984) 749
28. P. T. CHRISTOPHER and K. J. PARKER, *J. Acoust. Soc. Am.* **73** (1991) 1525
29. P. K. VERMA, V. F. HUMPHREY and F. A. DUCK, *Ultrasound Med. Biol.* **31** (2005) 1723
30. F. A. DUCK, *Physical Properties of Tissue* (London: Academic Press, 1990)
31. J. WU and J. TONG, *Ultrasound Med. Biol.* **24** (1997) 153
32. P. M. MORSE and K. U. INGARD, *Theoretical Acoustics* (New York: MacGraw-Hill, 1968)